Use of ISO 22157 Mechanical Test Methods and the Characterisation of Brazilian *P. edulis* bamboo

Christian Gauss[1], Holmer Savastano Jr.[2] and Kent A Harries[3]

Abstract

The characterisation of Brazilian *P. edulis* bamboo is presented as an example of the adoption of ISO 22157 test methods. Using digital imaging correlation (DIC), the behaviour of the bamboo material subject to mechanical tests, their interaction with boundary conditions, and the progression of damage during testing is illustrated. The DIC helped to identify and quantify specimen behaviour, particularly in the presence of a node. Nodes are shown to have a significant local effect on behaviour which can be mostly disregarded in compression and shear but are a weak link in tension. This behaviour is described as an artefact of the morphology of the bamboo fibres in the nodal regions. Specimen damage development was also described by DIC and the adoption of the limit of proportionality (LOP) as a measure of useful material capacity proposed. Additional recommendations related to the adoption of ISO 22157 are presented.

Keywords

Bamboo, Digital Image Correlation, *Phyllostachys edulis,* Test Methods

[1] PhD Candidate, University of Sao Paulo, Brazil; Visiting Scholar, University of Pittsburgh; gausschr@usp.br

[2] Professor, University of São Paulo; holmers@usp.br

[3] Professor, University of Pittsburgh; kharries@pitt.edu

1. Introduction

In 2004, the International Organisation for Standardisation (ISO) promulgated ISO 22157:2004 *Bamboo – Determination of physical and Mechanical Properties.* The development of this test methods Standard (ISO 22157-1:2004) and accompanying *Laboratory Manual* (ISO 22157-1:2004) had as its aim "to bring bamboo towards the level of an internationally recognised and accepted building material and engineering material… in favour of the well-being of lower income groups in developing countries, and in favour of a better environment in bamboo-growing countries." The development of ISO 22157:2004 initiated as early as 1988 and the initial draft, established in 1998 (INBAR 1999), was the work of a handful of dedicated individuals – who are dutifully acknowledged in the 2004 ISO Standard. The accompanying Laboratory Manual has as its aim "to give a practical 'how to do' explanation on how to perform tests according in the ISO 22157-1.". Since 2004, ISO 22157:2004 has been used internationally, formally adopted by at least eight[4] countries and anecdotally known to be used more broadly. While an imperfect measure of industry penetration and use, as of July 2019, Google Scholar identifies 291 citations on searches of "ISO 22157" and "ISO Standard 22157". In 2019, a significantly revised ISO 22157:2019 was published and the *Laboratory Manual* withdrawn.

ISO 22157:2004 includes four mechanical property tests: a) full-culm longitudinal compressive strength; b) longitudinal tensile strength using a "dogbone" specimen taken from the culm wall; c) flexural capacity based on a three-point bend test of a long length of culm; and d) longitudinal shear using the "bowtie test" (Janssen 1981). The Standard also provides guidelines for determining moisture content by drying, mass by volume, and shrinkage of bamboo.

The recently revised version, ISO 22157:2019, leveraged the considerable recent experience with bamboo materials which partially stemmed from the 2004 publication of ISO 22157. The 2019 revision added two mechanical property tests: e) tension perpendicular to fibres (Mitch et al. 2010); and f) bending perpendicular to fibres (so-called circumferential compression) (Sharma et al. 2012). In addition, moisture content by calibrated moisture meter and mass by culm length were added and existing mechanical tests (a) through d), above) were extensively revised. The 2004 method for determining shrinkage was withdrawn as a method that could not be practically performed.

Other mechanical test methods often used for bamboo materials but not [yet] included in ISO 22157 include g) interlaminar shear by tension (INBAR 1999; Moreira 1991); h) perpendicular shear (Cruz 2002); i) pin shear (Janssen 1981; Sharma 2010); j) flat-ring flexure (Virgo et al. 2018); and, k) small

[4] Colombia (NTC 5525), Ecuador (NTE INEN-ISO(DIS) 22157, Jamaica (JS ISO 22157), Vietnam (TCVN 8168), the Philippines (PNS ISO 22157), Netherlands (NEN-ISO 22157), Peru (Norma ISO/TC165/N315), India (IS 6874)

sample flexure (based on ASTM D7264 test method). A summary review of mechanical test methods a) through i) is provided in (Harries et al. 2012).

1.1 Selection of Bamboo Materials Test Methods

Those conducting material tests of bamboo may have limited access to complex test apparatuses. Nonetheless, "standard" testing needs to be just that: standard. Repeatability and minimising inter-laboratory variation to the greatest extent possible is critical so that a description of bamboo materials is as uniform as possible: creating a *lingua franca* among practitioners, as it were (Harries et al. 2019). Simple test methods are those that a) require minimal specimen preparation; b) do not require a complex test apparatus; and, c) are based on applying compression forces (Harries et al. 2012). Due to the dimensional variability and curved shape of bamboo, extracted test specimens are often not symmetric or require some of the material to be lost during specimen fabrication; in a functionally graded material such as bamboo, this may result in test specimens that do not represent the material as it is used *in situ*. Thus full-culm section specimens should be preferred for obtaining material properties reflective of *in situ* properties. A simple test apparatus will mitigate operator bias and accommodate the variable geometry of bamboo specimens. Finally, compression-based tests are simple to conduct and can often be carried out with quite fundamental instrumentation (Glucksman and Harries 2015). Tension-based tests, on the other hand, require fixtures to interface with the highly anisotropic bamboo that can bias test results.

1.2 Objectives of Study

The objective of this paper is to describe the use of bamboo material characterisation tests and identify some factors affecting the performance of these. Using digital image correlation (DIC), the behaviour of the tests specimens, their interaction with boundary conditions, and the progression of damage during testing is illustrated. Understanding specimen behaviour will lead to more robust mechanical testing practice. In addressing these objectives, an example of the mechanical characterisation of a batch of Brazilian *P. edulis* is described.

2. Bamboo Materials

Phyllostachys edulis (Moso) bamboo was obtained from a supplier near Sao Paulo, Brazil. Approximately 140 culms between 3 and 5 years of age were harvested and subsequently treated (as described by Gauss (2019)) from which 4 m long poles were extracted. The diameters ranged from 80 to 100 mm, wall thickness from 6 to 9 mm and the average oven-dry density prior to treatment was 760 kg/m^3. Image analysis determined an average fibre bundle content of 29%. The bamboo reported in this study was also subject of a study of treatment processes (Gauss 2019). The specimens were treated in one of the following manners:

- culms were treated with chromated copper borate (CCB) in a pressure vessel using a vacuum (-600 mmHg for 30 min.) – pressure (10 kgf/cm^2 for 60 min.) – vacuum (-600 mmHg for 30 min.) process.
- culms were treated by seven- to ten-day immersion in an 8% concentration of agricultural grade disodium octaborate tetrahydrate (DOT).

Description of the treatment study is presented in Gauss et al. (2019). Analysis of variation (ANOVA) of all data indicated that the effect of the treatment conditions had no significant effect on the mechanical properties of bamboo. All mechanical properties reported in this study were found to fall within the 95% confidence interval band and have a normal distribution irrespective of treatment. Therefore, in support of the objectives of this paper, data from the treatment processes have been combined. The density of the treated *P. edulis* specimens was found to be 810 kg/m^3 (COV = 0.05), also using the method of ISO 22157:2019. For all tests, moisture content at the time of testing was determined using the oven-method of ISO 22157:2019 and ranged from 7% to 10%.

3. Test Methods

Test specimen sampling was random within the batch described (resulting in 17 poles from the batch of 140). Full culm section specimens were used for compression and shear tests while machined coupons were used for tension and small coupon bending.

3.1 Full culm compression parallel to fibres

Full culm compression tests based on that prescribed by ISO 22157:2019 were conducted. Apart from some minor revisions (none affecting the samples tested in this study), the conduct of this test is the same as ISO 22157:2004. ISO 22157 specifies "The length of the specimen shall be taken as the lesser of the outer diameter, *D*, or 10 times the wall thickness, 10t. For the *P. edulis* specimens reported these values were essentially the same: the average values of *D* and *t* of the compression specimens were 78.3 mm (COV = 0.04) and 7.23 mm (COV = 0.09), respectively. For this study, specimen length (77.9 mm; COV = 0.04) was taken as the culm diameter, in all cases. ISO 22157:2019 requires an "intermediate layer" be placed at both ends of the specimen in order to minimise friction, causing radial restraint of the specimen ends. Compliant with ISO 22157:2019, sulphur 'capping compound' was used as shown in Figure 1a. Applied load was determined from the test machine load cell and all other strain data was determined using digital image correlation (DIC) techniques described below. A total of 55 specimens, 41 internode and 14 with a node at their mid height, were tested.

Compression strength parallel to the fibres is calculated from test results as:

$$f_c = P/A_{culm} \quad [1]$$

In which P is the applied axial load and $A_{culm} = \pi/4 \times [D^2 - (D - 2t)^2]$ is the cross sectional area of the culm. Compression modulus, E_c, is determined from DIC analysis.

3.2 Full culm shear parallel to fibres

The so-called 'bowtie' shear test was developed by Janssen (1981) and is standardised in ISO 22157:2019. Apart from a minor revision (again, not affecting the samples tested in this study) this test is identical to the ISO 22157:2004. In this test (Figure 1b), the full culm specimen (having the same dimensional requirements as the compression test) is supported at its lower end over two opposing quadrants, and loaded at its upper end over the other two opposing quadrants. In this manner, loading the specimen results in four shear areas (a typical failure is seen in Figure 1b). Specimens were generally sampled immediately adjacent compression specimens, therefore dimensions are essentially identical: average specimen length was 77.3 mm (COV = 0.03) and diameter and culm thickness were 78.1 mm (COV = 0.03) and 7.28 mm (COV = 0.08), respectively. Applied load was determined from the test machine load cell and all other strain data was determined using DIC. A total of 49 specimens, 36 internode and 13 with a node at their mid height, were tested.

Shear strength parallel to the fibres is calculated from test results as:

$$f_v = P/4Lt \qquad [2]$$

In which P is the applied load and $L \times t$ is the area of each shear plane (L is specimen length and t is culm wall thickness). The test is controlled by the first shear plane to fail and therefore f_v is interpreted as the lower bound shear strength. Shear modulus, G, is determined from DIC analysis.

3.3 Tension parallel to fibres test

Significant revisions were made to the ISO 22157 tension test between 2004 and 2019. In ISO 22157:2019 the specimen orientation as it is cut from the culm and subsequently tabbed is specified (as seen in Figure 1c). Additionally, rotationally-restrained boundary conditions of the test machine were as specified in ISO 22157:2019. Both specimen orientation and boundary conditions were shown by Richard and Harries (2015) to significantly impact tension test results due to the graded nature of the culm wall. ISO 22157:2019 standardises these parameters; the present tests are compliant with ISO 22157:2019.

Specimens were extracted from culm walls as shown in Figure 1c. The average wall thickness, t = 7.07 mm (COV = 0.10) and the average specimen breadth, b = 2.68 mm (COV = 0.16). All specimens were 200 mm long and had a gauge length of 100 mm as shown in Figure 1c. Applied load was determined from the test machine load cell. In addition to DIC, an external 50 mm gauge length extensometer (seen in Figure 1c) was used to determine tensile modulus and validate DIC data. A total of 84 specimens, 57 internode and 27 with a node in the middle of the gauge length, were tested.

Tension strength parallel to the fibres is calculated from test results as:

$$f_t = P/A \quad [3]$$

in which P is the applied axial load and $A = bt$ is the cross-sectional area of the gauge length of the specimen. Tension modulus, E_t, is determined from DIC analysis or using an external extensometer as:

$$E_t = \Delta f_t/\Delta \varepsilon \quad [4]$$

Where the change in stress (f_t) and measured strain (ε) is taken only between two points in the elastic region of behaviour (i.e., below any observed limit of proportionality).

3.4 Small coupon bending

ISO 22157 promulgates a full-culm bending test but not a small coupon bending test. The full-culm test can be difficult to conduct – requiring a long specimen (a minimum span length of 30*D* is prescribed) which corresponds to large deflections requiring a versatile test arrangement and a series of 'saddles' to conduct the test. Additionally, ISO 22157 is silent on how taper (*D* and/or *t*) over the long specimen length should be limited and how this will affect results. Richard et al. (2017) argue that even at a length of 30*D*, the ISO 22157 full-culm flexure test does not determine modulus of rupture, but rather the member flexural capacity of the culm being tested. This capacity is rarely governed by compression or tension behaviour but is most always governed by longitudinal shear of the culm in flexure which itself is a mixed mode of failure due to the stress state of the culm. Trujillo et al. (2017) proposed that the full-culm flexure test is appropriate for grading schema (ISO 19624:2018) based on member capacity. Nonetheless, the test does not provide a meaningful stress that may be used in a stress-based design.

For these reasons, like some other researchers (e.g., Gottron et al. 2014; Richard et al. 2017), a small coupon flexural test is adopted. In the longitudinal direction, bamboo is often described as a unidirectional fibre-reinforced material. For this reason, *ASTM D7264 – 15 Standard Test Method for Flexural Properties of Polymer Matrix Composite Materials* was adopted. A three-point bending test (Figure 1d; ASTM D7264 Procedure A) was selected in order to maximise the test shear span and therefore minimise the effects of shear.

Bending specimens were extracted from culm walls as shown in Figure 1c. However, for flexure, *b* is greater than *t* and bending is about an axis perpendicular to the dimension *t*. Due the curvature of the culm wall, the coupons are sanded flat in their through-thickness direction. The average resulting specimen dimensions were, t = 6.57 mm (COV = 0.08) and b = 9.95 mm (COV = 0.06). Coupons were 200 mm long and tested in three-point bending over a span length of 160 mm. The average shear span to depth ratio exceeded 10 in every test (average was 12.3 (COV = 0.09)); this exceeds the minimum recommended ratio of 8 (ASTM D7264).

Two test orientations are possible (Figure 1d) resulting the outer culm wall being in compression (OC) or in tension (OT); 54 tests of the former and 10 of the latter were conducted. In addition, 24 specimens having a node at midspan were tested; these were conducted in the OC orientation in every case.

The modulus of rupture based on an assumption of a homogeneous material is determined as:

$$f_r = 3PL/2bt^2 \qquad [5]$$

Where P is the maximum applied load at midspan, L is the simple test span and b and t are specimen width and depth, respectively.

The apparent axial modulus of the homogeneous specimen derived from bending, E_f, is determined from the midspan displacement, Δ. For three-point bending:

$$E_f = PL^3/4\Delta bt^3 \qquad [6]$$

More complex analysis of the test is possible using data from DIC; this will be described in the discussion of results, below.

3.5 Digital image correlation

Digital image correlation (DIC) is a well-established contact-free means of obtaining full-field surface deformations (and therefore strains). Specimens are painted with a speckle pattern prior to testing (photocopier toner broadcast onto wet white spray paint, the result is seen in Figure 1a). During the test, consecutive high-resolution images (2448 x 2049 pixels) are taken every 0.5 sec. and deformation patterns (based on sampling of the speckle pattern) are recorded. Post-processing allows relative displacements and specified strain fields to be obtained in three dimensions. The system used in this study is a VIC-3D dual camera system and DIC processing software (Correlated Solutions). The advantage of a dual camera system when viewing full-culm bamboo is that the strain field can be accurately obtained on the curved surface of the bamboo. The resolution of DIC data is a function of the field of view and camera resolution. For the small material samples tested in this study, theoretical strain resolution better than 1 microstrain is obtained; nonetheless strains are reported with a precision of 10 microstrain. Subsequent figures show a variety of DIC-obtained images that will be discussed below.

4. Test Results

ANOVA analysis of all data (Gauss 2019) indicated that mechanical properties reported in this study were found to fall within the 95% confidence interval band for having a normal distribution.

4.1 Full culm compression parallel to fibres

A summary of full culm compression test results is given in Table 1. Representative compressive stress versus strain data is shown Figure 2a. The strain shown in Figure 2 is obtained by DIC as the axial (longitudinal) strain 'averaged' over a vertical section (shown by dotted lines in Figures 2b and 2c). As is typical with a correctly executed test, the stress-strain behaviour shown in Figure 2a is essentially linear to failure. The strain fields at lower load levels are uniform over the specimen. As the stress approaches ultimate, restraint from the loading platens results in larger axial strains near the middle of the specimen (Figure 2b); typically, the specimen will bulge-out at this location and eventually split. Once split, the slope of the compression stress-strain curve (i.e. compression stiffness) will typically become negligible (Figure 2a, post peak behaviour). The effect of the initiation of splitting is seen in Figure 2b: near the bottom of the specimen to the right of the dotted line, a small region of low axial strain is forming. Nonlinear behaviour may also result from uneven loading of the culm end; this was generally not seen in this study since sulphur capping compound was used. Using a sulphur capping compound (as is used for testing reinforced concrete cylinders) largely addresses uneven loading as the capping results in uniform distribution of force to the culm and, if done correctly, results in parallel specimen end surfaces. The capping compound provides a low friction interface and relatively little lateral restraint from the thin layer of material. To minimise restraint, once capped, the capping material covering the culm annulus can be broken away leaving only the culm walls capped.

The limit of proportionality (LOP) is defined as the limit of observed elastic behaviour (see Figure 2a for example). A relatively high LOP indicates a good test procedure likely to yield a representative value of bamboo compression strength. As described above, behaviour beyond the LOP, is indicative of other mechanisms of failure.

As shown in Table 1, neither compression capacity, modulus of elasticity or LOP are affected by the presence of a node. Indeed, considering the natural variation present, tests with and without nodes cannot be statistically distinguished (see unpaired t-test *p*-values shown in Table 1). Locally, however, the node is seen to be stiffer than the surrounding internode region. As seen in Figure 2c, the local compressive strain at the node is to about one half the average strain over the height of the specimen. The behaviour affected by the presence of the node is discussed further below.

4.2 Full culm shear parallel to fibres

A summary of shear test results is given in Table 2. Representative shear stress versus strain data is shown Figure 3a. The strain shown in Figure 3 is obtained by DIC along one of the four shear planes. At lower stress levels, the shear strain is relatively uniformly distributed along the height of the specimen. Similar to compression tests, as the LOP is exceeded, the shear strains tend to increase near the loading platens where the shear cracks and eventual failures initiate. This behaviour results from the stress concentrations at the edges of the loading platens and is clearly seen in Figure 3b where the strain at the top and bottom of the specimen is about 40% greater than at mid-height. Due to this stress concentration, the LOP is lower in the shear tests than in compression. Also similar to the compression tests, the presence of the node has no significant effect on the measured capacity (*p*-values, Table 2) and a stiffening effect on the local shear response (Figure 3c).

4.3 Tension parallel to fibres test

A summary of tension test results is given in Table 3. Representative tension stress versus strain data is shown Figure 4a. The preference for the through-culm wall orientation tested using rotationally-restrained boundary conditions (Richard and Harries 2015) is evident in Figure 4a. There is no apparent strain gradient across or along the 100 mm gauge length. The solid data points in Figure 4b, showing the axial strain along the middle 40 mm gauge length indicate some variation but no gradient along the gauge length. The efficacy of the DIC data is validated by the data from the external extensometer from which the average strain over a 50 mm gauge length is determined. the behaviour is essentially linear to a brittle failure; there is no marked difference between LOP and failure. This lack of nonlinearity – even near failure – indicates a failure dominated by fibre rupture. The effect that the presence of a node has on the tension behaviour is dramatic. In this study, the tensile capacity with a node is approximately 36% of the internode counterpart. While stiffness over the gauge length (including the node) is reduced, the local stiffness of the node itself is significantly lower. As seen in Figure 4b, the strain at the node increases about four times over the strain in the adjacent internodes. The behaviour affected by the presence of the node is discussed further below.

4.4 Small coupon bending

A summary of coupon bending test results is given in Table 4; these results assume gross sections properties and homogenous material properties and should be interpreted as being 'average' properties for a cross section. Representative flexural stress versus extreme fibre strain data is shown in Figure 5a. Bending behaviour is clearly different for OC and OT orientation (*p*-values in Table 4) and the behaviour is more nonlinear (especially for OT); having a lower LOP than previous tests types. As an additional measure of this behaviour, the cumulative energy (or specific energy), *SE*, taken as the area under the stress-extreme fibre strain curve is also given in Table 4.

From extreme fibre strains, shown in Figure 5b, the behaviour of the specimens becomes evident. For both OC and OT specimens, flexure is described by a softer nonlinear response of the compression zone and a stiffer tension behaviour having a higher LOP. The greater nonlinearity observed in the compression strains indicates more local damage in the matrix-dominated compression zone. Compression behaviour drives the failure of OT specimens which are generally unable to develop large tensile strains despite the culm wall being oriented such that the greater fibre density is in tension. Based on observation, it appears that OC specimen failure is driven by excessive tensile strains resulting in failure of the relative lightly ‘fibre reinforced’ tension zone. Bending tests having a node a midspan are very clearly dominated by the poor tensile behaviour of the node as is discussed below.

4.4.1 Assessing “Real” Bending Behaviour

The difference in tensile and compression behaviour in flexure results in a shift in the neutral axis of the specimen toward the stiffer outer culm wall; this is illustrated in Figures 5c and 5d for representative OC and OT specimens, respectively. This shift reflects the differences in compressive and tensile stiffness resulting from a) the varying fibre density in the culm wall; and b) the different tension and compression behaviour associated with the fibres themselves. If the strain distribution through the culm wall can be determined as is the case using DIC, the actual behaviour of the culm wall in flexure can be determined. Assuming a linear strain distribution (Figures 5c and 5d), the moment applied to the coupon, M, is resisted by a tension-compression couple having a lever arm equal to (2/3)t. From equilibrium, and the recorded extreme fibre strains, ε_T and ε_C, the tensile and compression moduli can be determined:

$$E_{TF} = 3M/t\bar{y}\varepsilon_T \qquad [7]$$

$$E_{CF} = 3M/t(t - \bar{y})\varepsilon_C \qquad [8]$$

Where $\bar{y} = t\varepsilon_T/(\varepsilon_T - \varepsilon_C)$ is the location of the neutral axis (relative to the tensile face of the coupon). The approach using Equations 7 and 8, however is effected by a number of test parameters and is only practical when sufficiently robust strain data is available. In three-point flexure, the recorded strain at the compression face is significantly impacted by local deformation caused by the application of the load and local strains in this region are unreliable. Using four-point flexure, having a constant moment region, addresses this issue but such tests are limited by available internode length and the need to have a shear span to depth ratio greater than 8. The utility of E_{TF} and E_{CF} in practice is also limited. For this reason, the use of f_r (Eq. 5) is believed sufficient to represent the flexural behaviour of small coupon bending samples.

5. Effect of Node

In compression and shear, the presence of a node in the test specimen has a local stiffening effect. This is attributed to the reduction in unidirectional fibre alignment and the thickening of the culm wall in the nodal region (Figure 6). In the node, the bamboo fibres are shorter (Liese 1998) than in the internode. Additionally, as many fibre bundles simply pass through the node, others rearrange themselves into the sheath (outwards) and diaphragm (inwards) (Liese 1998). Liese illustrates the rearrangement of the vessels (vascular anastomoses) in the nodal region (Figure 6); the ‘vascular skeleton’ supporting the primary vessels also becomes more isotropic. The total fibre volume in *P.*

edulis is typically less than 30% and, in general, fibre volume in other species rarely exceeds 40% (Akinbade et al. 2019). As a result, both compression and shear in the longitudinal direction are matrix-dominated behaviours. As the fibres become less unidirectionally aligned in the node, there is a natural stiffening effect as fibres now reinforce the weaker parenchyma matrix in directions other than longitudinal. The additional section thickness at the node further reinforces the behaviour resulting in a stiffer response. The local stiffening effect has no statistically significant effect on the global, or specimen stiffness as illustrated in Tables 1 and 2.

The same bamboo node morphology results in a softening of the fibre-dominated tension behaviour; this is evident in Table 3 and Figure 4, reporting direct tension results. However, the same mechanism also drives the small coupon bending tests in which a node is included. The presence of the node dominates the tension behaviour of the flexural specimen leading to a brittle failure. Unlike in compression, in tension the node becomes a 'weak link'. The strains shown in Figure 5b illustrate this dramatically, where then tension strain increases essentially unbounded while the compression strain has considerable reserve capacity (In Figure 5b, the compression strain has barely achieved half that observed in the OC or OT specimens without a node).

6. Characteristic Properties of *P.edulis*

The average mechanical properties determined for the Brazilian *P. edulis* tested are summarised in Table 5 and shown (indicating one standard deviation) in Figure 7. In Table 5 these are compared to other such data reported in the literature and seem to be in general agreement. The characteristic design strengths that resulted from this study are also summarised in Table 5. These values are defined as the 5th percentile value determined with 75% confidence (ISO 22156:2004; ISO 22156:2019) and are calculated for data having a normal distribution as:

$$f_{ik} = f_{i\,average} - K \times \text{standard deviation of } f_i \qquad [9]$$

Where *K* is the confidence level factor associated with the confidence interval (75%), data percentile (5%) and the number of samples tested (*n*). Values of *K* are tabulated in multiple sources; the tables included in ASTM D2715 were used in the present study. For a test series having $n = 50$, $K = 1.811$.

Stiffness values used in design are conventionally the mean value established with 75% confidence (ISO CD 22156:2019) calculated for data having a normal distribution as:

$$E_{ik} = E_{i\,average} - 1.15 \times \text{standard deviation of } E_i \qquad [10]$$

The characteristic values apply only to the batch of *P. edulis* tested. The relatively high characteristic values reflect the low variation observed in the tests. Coefficient of variation (COV) for both strength and modulus of elasticity remained below 0.11 in all performed tests. The process of testing illustrated in this paper reflects what is required to establish characteristic design values which may be then used to grade the batch of bamboo (ISO 19624:2018).

6.1 Minimising Material Damage in Bamboo Design

While the characteristic values of strength are conventionally used in design (ISO 22156:2004; ISO CD 22156:2019), the application of the limit of proportionality (LOP) may be more appropriate since exceeding this limit is associated with damage and material degradation. Additionally, stipulating the LOP as the design value of interest is consistent with the use of the modulus of elasticity which is calculated at strains below the LOP. The average LOP values and associated characteristic values (Eq. 9) are summarised in Table 5. The authors argue, that these are the appropriate values of stress for use in design.

7. Conclusions and Recommendations

The characterisation of Brazilian *P. edulis* bamboo is presented as an example of the adoption of ISO 22157 test methods. The efficacy of and parameters affecting the test specimen behaviour were investigated using digital image correlation (DIC) techniques. The DIC helped to identify and quantify specimen behaviour, particularly in the presence of a node. In particular, nodes are shown to have a significant local effect on behaviour. In compression and shear, the presence of a node has little impact. In tension, however, the node is a 'weak link' significantly reducing the available capacity of the culm. This behaviour is an artefact of the morphology of the bamboo fibres in the nodal regions. Specimen damage development was also described by DIC and the adoption of the limit of proportionality (LOP) was proposed as a measure of useful material capacity.

7.1 Recommendations for Testing Mechanical Properties of Bamboo

While this study has demonstrated the efficacy of using DIC, such instrumentation is available to only a handful of bamboo researchers and is not presently suitable for field implementation. Nonetheless, the observations made using DIC can inform bamboo materials testing practice. The following recommendations are made.

1. In addition to ultimate capacity, the limit of proportionality (LOP) should be reported for all tests. This requires a measure of either specimen displacement or strain. Absent such a method, machine cross head travel can be used as a surrogate for displacement sufficient to identify the LOP. Machine cross head travel should never be used to calculate a real displacement, strain or modulus however.
2. Full-culm compression and 'bowtie' shear tests parallel to the fibres are relatively insensitive to the presence of a node. ISO 22157:2019 prescribes that both tests use 50% samples including a node to establish characteristic values. While reasonable, a small degree of conservativeness will result if values are determined for a sample containing no nodes.
3. The ISO 22157:2019 tension test has not been validated considering the new restrictions placed on specimen orientation and boundary conditions. In the present study – enforcing these

restrictions – relatively low variability (COV = 0.11) was observed. Some issues with the tabs affecting test performance were observed; further investigation of alternative tension tab arrangements and materials is required to improve the utility of this test method.

4. The ISO 22157:2019 tension test also specifies that specimens contain one node in the gauge length. This will result in conservative values of tension strength (Table 3). However, the relatively local effect of the node (Figure 4b) will make strains and modulus of elasticity obtained from this test unreliable and a function of the gauge length used. While bamboo tensile strength is conservatively represented in the presence of a node, modulus of elasticity may be unrealistically low. In this perspective, the utility of the ISO 22157 tension test requires further investigation.
5. Although beyond the scope of the present study, researchers and practitioners are reminded that it is critical to report bamboo density and moisture content since both of these parameters are well known to affect material properties.

Small coupon bending of bamboo specimens has been demonstrated applying a method used for reinforced plastics, ASTM D7264 (Procedure A: three-point bending). It is proposed that a similar method be adopted into ISO 22157. The small coupon geometry is appropriate for determining the material properties for bamboo intended to be used in engineered products such as glue-laminated bamboo or cross laminated bamboo timbers. In such applications, bamboo strip orientation should be randomised, therefore standardising the bending test in the OT orientation will result in uniformly conservative design values. It is not believed that the inclusion of a node is necessary in bending tests.

If strain data is to be determined or data beyond that derived from Equations 5 and 6 is necessary, four-point bending (ASTM D7264 Procedure B) is required in order to establish a constant moment region unaffected by the application of load. However, maintaining the geometry of the four-point bend specimen while also ensuring that the shear span remain greater than $8t$ requires a test specimen that is at least $32t$ long. This may be impractical for many species considering the internode length available. Further development of a small coupon flexural test for bamboo is recommended.

Acknowledgements

This research was partially supported through National Science Foundation Award 1634739 *Collaborative Research: Full-culm Bamboo as a Full-fledged Engineering Material*. The authors acknowledge the support of National Council for Scientific and Technological Development (CNPq Process #307723/2017-8) and São Paulo Research foundation, FAPESP Grant No 2018/18571-8 and 2016/26022-9, which supported the first author's work at the University of Pittsburgh and the University of São Paulo.

References

Akinbade, Y., Harries, K.A., Flower, C., Nettleship, I., Papadopoulos, C., and Platt, S.P. (2019) Through-Culm Wall Mechanical Behaviour of Bamboo, Construction and Building Materials, **216**, 485-495.

ASTM D2915-17 Standard Practice for Sampling and Data-Analysis for Structural Wood and Wood-Based Products, ASTM International, West Conshohocken PA USA.

ASTM D7264 – 15 Standard Test Method for Flexural Properties of Polymer Matrix Composite Materials, ASTM International, West Conshohocken PA USA.

Cruz, M.L.S. (2002) *Caracterização fisica e mecânica de colmos inteiros do bambu da espécie phyllostachys aurea: comportamento à flambagem* [Physical and mechanical characterization of whole stems of phyllostachys aurea bamboo: buckling behaviour]. Master's Thesis, Pontifícia Universidade Católica – Rio de Janeiro, 114 pp (in Portuguese).

Deng, J., Chen, F., Wang, G. and Zhang, W. (2016) Variation of Parallel-to-Grain Compression and Shearing Properties of Moso Bamboo Culm , *BioResources*. **11**, 1784–1795.

Dixon, P.G., Ahvenainen, P., Aijazi, A.N., Chen, S.H., Lin, S., Augusciak, P.K., Borrega, M., Svedström, K. and Gibson, L.J., (2015) Comparison of the structure and flexural properties of Moso, Guadua and Tre Gai bamboo, *Construction and Building Materials* **90**, 11–17.

Gauss, C. (2019) *Preservative treatment and chemical modification of bamboo for structural purposes*, PhD Dissertation, University of Sao Paulo.

Gauss, C., Harries, K.A., Kadivar, M., Akinbade, Y. and Savastano, H. (2019) Quality assessment and mechanical characterization of P. edulis bamboo treated with CCB and DOT, *Holzforschung* (in review)

Glucksman, B., and Harries, K.A. (2015) In-the-Field Test Methods for Bamboo – The test-kit-in-a-backpack, Proceedings 15th International Conference Non-conventional Materials and Technologies (NOCMAT 15), Winnipeg, Canada. August 2015.

Gottron, J. Harries, K. and Xu, Q. (2014) Creep Behaviour of Bamboo, *Journal of Construction and Building Materials*, **66**, 79–88.

Habibi, M.K., Samaei, A.T., Gheshlaghi, B., Lu, J. and Lu, Y. (2015) Asymmetric flexural behaviour from bamboo's functionally graded hierarchical structure: Underlying mechanisms, *Acta Biomaterialia* **16**, 178–186.

Harries, K.A., Ben Alon, L. and Sharma, B. (2019) Chapter 4: Codes and Standards Development for Nonconventional and Vernacular Materials. In *Nonconventional and Vernacular Construction Materials: Characterisation, Properties and Applications*, 2nd edition. K.A. Harries and B. Sharma, editors. Woodhead (Elsevier) Publishing Series in Civil and Structural Engineering.

Harries, K.A., Sharma, B. and Richard, M.J. (2012). Structural Use of Full Culm Bamboo: The Path to Standardisation, *International Journal of Architecture, Engineering and Construction*. **1**(2), 66-75.

Huang, X. Hse, C.Y. and Shupe, T.F. (2015) Study of moso bamboo's permeability and mechanical properties, ICE Emerging Materials Research **4**, 130–138.

INBAR (1999) *An International Model Building Code for Bamboo*. Janssen, J.J.A (editor). The International Network on Bamboo and Rattan, Beijing.

ISO CD 22156:2019 Bamboo – Structural Design, International Organization for Standardization, Geneva. [Committee Document: ongoing revisions to ISO 22156:2004, expected publication in 2021]

ISO 22156:2004 Bamboo – Structural Design, International Organization for Standardization, Geneva.

ISO 22157:2019 Bamboo structures -- Determination of physical and mechanical properties of bamboo culms -- Test methods, International Organization for Standardization, Geneva.

ISO 22157-1:2004 Bamboo -- Determination of physical and mechanical properties -- Part 1: Requirements [withdrawn], International Organization for Standardization, Geneva.

ISO/TR 22157-2:2004 Bamboo -- Determination of physical and mechanical properties -- Part 2: Laboratory manual [withdrawn], International Organization for Standardization, Geneva.

ISO 19624:2018 Bamboo structures -- Grading of bamboo culms -- Basic principles and procedures, International Organization for Standardization, Geneva.

Janssen, J. (1981) *Bamboo in Building Structures*. Doctoral Dissertation, Eindhoven University of Technology, Netherlands.

Liese, W. (1998) *The Anatomy of Bamboo Culms*, Brill, 204 pp.

Mitch, D., Harries, K.A., and Sharma, B. (2010) Characterization of Splitting Behavior of Bamboo Culms, *ASCE Journal of Materials in Civil Engineering*, **22**(11), 1195-1199.

Moreira, L.E. (1991) *Desenvolvimento de estruturas treliçadas espaciais de bamboo* [Development of bamboo space trusses]. Doctoral Dissertation, Pontifícia Universidade Católica – Rio de Janeiro, (in Portuguese).

Richard, M., Gottron, J., Harries, K.A. and Ghavami. K. (2017) Experimental Evaluation of Longitudinal Splitting of Bamboo Flexural Components, *ICE Structures and Buildings Themed issue on bamboo in structures and buildings*, **170**(4), 265-274.

Richard, M.J., Harries, K.A., (2015) On Inherent Bending in Tension Tests of Bamboo, *Wood Science and Technology* **49**(1), 99-119.

Sharma, B. (2010) *Performance Based Design of Bamboo Structures*. Doctoral Dissertation, University of Pittsburgh, 201 pp.

Sharma, B., Harries, K.A. and Ghavami, K. (2012) Methods of Determining Transverse Mechanical Properties of Full-Culm Bamboo, *Construction and Building Materials*, **38**, 627-637.

Trujillo, D., Jangra, S. and Gibson, J. (2017). Flexural properties as a basis for bamboo strength grading, *ICE Structures and Buildings Themed issue on bamboo in structures and buildings*, **170**(4), 284-294

Virgo, J., Moran, R., Harries, K.A., Garcia, J.J. and Platt, S. (2018) Flat Ring Flexure Test for Full-Culm Bamboo, *Materials Research Proceedings*, **7**, 349-358.

Xu, Q. Harries, K.A., Li, X, Lui, Q and Gottron, J. (2014) Mechanical properties of structural bamboo following immersion in water, *Engineering Structures* **81**(15), pp 230-239.

Yu, H.Q., Jiang, Z.H., Hse, C.Y., and Shupe T.F. (2008) Selected physical and mechanical properties of moso bamboo (phyllostachys pubescens), *Journal of Tropical Forest Science* **20**, 258–263.

Table 1 Full culm compression parallel to fibre test results.

	Internode specimen			Specimen with node			p-value	All specimens		
	n	average	COV	n	average	COV		n	average	COV
f_c, MPa	41	57.5	0.09	14	59.5	0.06	0.19	55	57.9	0.08
E_c, MPa		20,300	0.10		20,640	0.12	0.61		20,380	0.10
LOP, MPa		50.9 $0.89f_c$	0.10		50.7 $0.85f_c$	0.10	0.90		50.7 $0.88f_c$	0.10
NOTES:	Moisture content = 10.2% (COV = 0.04) Specimens sampled from 17 different culms p-value from unpaired t-test comparing internode specimens to specimens with nodes									

Table 2 Full culm shear parallel to fibre test results.

	Internode specimen			Specimen with node			p-value	All specimens		
	n	average	COV	n	average	COV		n	average	COV
f_v, MPa	36	18.0	0.08	13	18.1	0.07	0.83	49	18.1	0.08
G, MPa		2850	0.10		2790	0.10	0.52		2830	0.10
LOP, MPa		12.2 $0.68f_v$	0.09		12.2 $0.67f_v$	0.10	1.00		12.2 $0.67f_v$	0.10
NOTES:	Moisture content = 10.3% (COV = 0.04) Specimens sampled from 16 different culms p-value from unpaired t-test comparing internode specimens to specimens with nodes									

Table 3 Tension parallel to fibre test results.

	Internode specimen			Specimen with node			p-value
	n	average	COV	n	average	COV	
f_t, MPa	57	275	0.11	27	100	0.20	0.0001
E_t, MPa		17,470	0.09		11,190	0.18	0.0001
NOTES:	Moisture content = 6.8% Specimens sampled from 11 different culms p-value from unpaired t-test comparing internode specimens to specimens with nodes						

Table 4 Coupon flexure test results.

	Internode specimen outer culm wall in compression (OC)			Internode specimen outer culm wall in tension (OT)			p-value	Specimen with node at midspan		
	n	average	COV	n	average	COV		n	average	COV
f_R, MPa	54	205	0.06	10	183	0.08	0.0001	24	127	0.11
E_R, MPa		16,320	0.06		15,570	0.06	0.03		15,050	0.07
SE, kJ/m^2		39.5	0.13		78.5	0.23	0.0001		13.6	0.23
LOP, MPa		124 $0.61f_R$	0.06		67 $0.37f_R$	0.15	0.0001		87 $0.68f_R$	0.11
NOTES:	Moisture content = 7.3% (COV = 0.09) Specimens sampled from 11 different culms p-value from unpaired t-test comparing OC specimens to OT specimens									

Table 5 Comparison with *P.edulis* data available in literature.

source	ρ	MC	f_c	E_c	f_v	G	f_t	E_t	f_r	E_r
	kg/m^3	%	MPa	MPa	MPa	MPa	MPa	MPa	MPa	MPa
this study strength	810	7-10	57.9	20,380	18.1	2830	275 (no node) 100 (node)	17,470 11,190	205 (OC) 183 (OT)	16,320 15,570
this study LOP			50.7		12.2				124 (OC) 67 (OT)	
this study characteristic strength			49.5	18,040	15.4	2520	220 (no node) 63 (node)	15,660 8874	183 (OC) 152 (OT)	15,190 14,490
this study characteristic LOP			41.5		10.0				110 (OC) 49 (OT)	
Akinbade et al. (2019)	896	14	48.1	-	15.1	-	-	-	-	-
Deng et al. (2016)	655	8-12	-	-	11.8	-	48 (node)	-	-	-
	799		-	-	15.9	-	62 (node)	-	-	-
Dixon et al. (2015)	400	4	-	-	-	-	-	-	52	4350
	850		-	-	-	-	-	-	215	16,680
Habibi et al. (2015)	-	-	-	-	-	-	-	-	146 (OC) 125 (OT)	11,400 9,900
Huang et al. (2015)	-	12	61.3	-	12.9	-	197 (no node)	-	149	-
Xu et al. (2014)	-	10	46.0	11200	11.2	-	-	-	-	-
Yu et al. (2008)	703	10	-	-	-	-	168 (no node)	16,400	-	-

a) compression specimen showing sulphur capping and DIC speckle pattern. Specimen height is approximately 90 mm.

b) “bowtie” test set-up and typical specimen failure. Specimen height is approximately 90 mm.

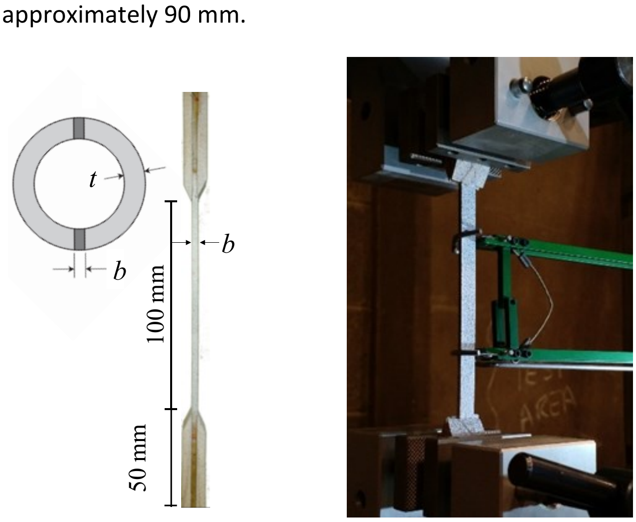

c) test specimen geometry and test set-up showing DIC speckling and extensometer

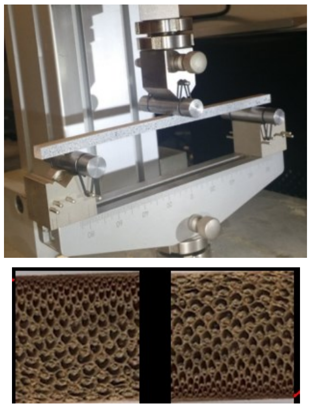

Outer culm wall in compression (OC)

Outer culm wall in tension (OT)

d) three point bending test of coupon and specimen orientation. Flexural span is 160 mm and specimen depth is approximately 7 mm

Figure 1 Bamboo test methods.

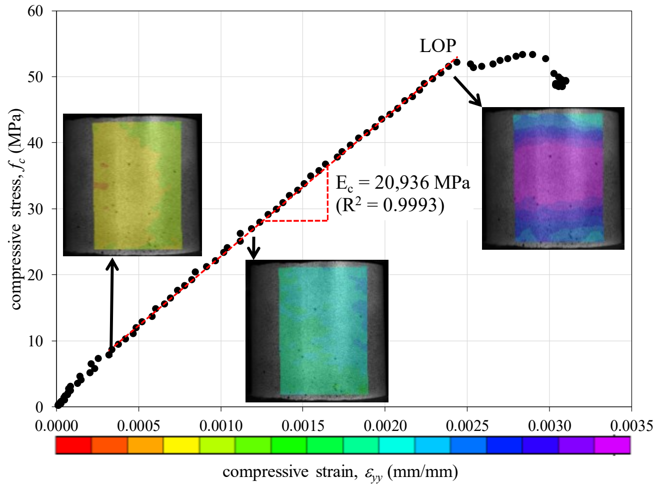

a) longitudinal stress-strain progression of internode compression test

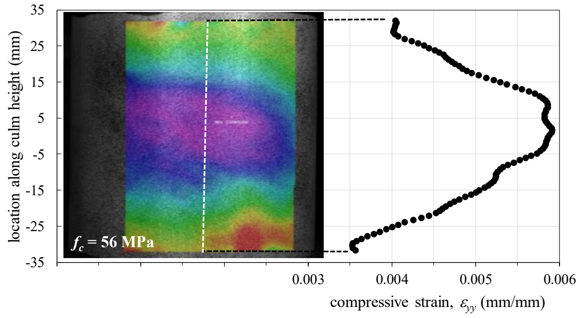

b) longitudinal strain distribution in internode specimen at stress = 56 MPa

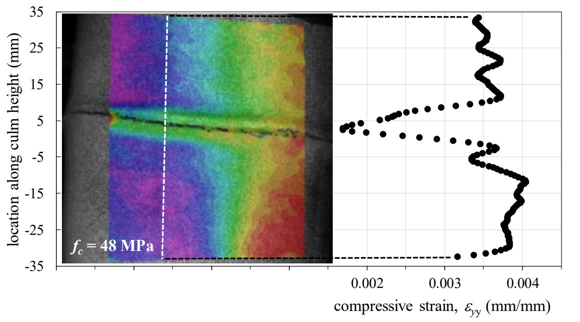

c) longitudinal strain distribution in specimen with node at stress = 48 MPa

Figure 2 Representative results of longitudinal full-culm compression test (compressive strain shown as positive in this figure).

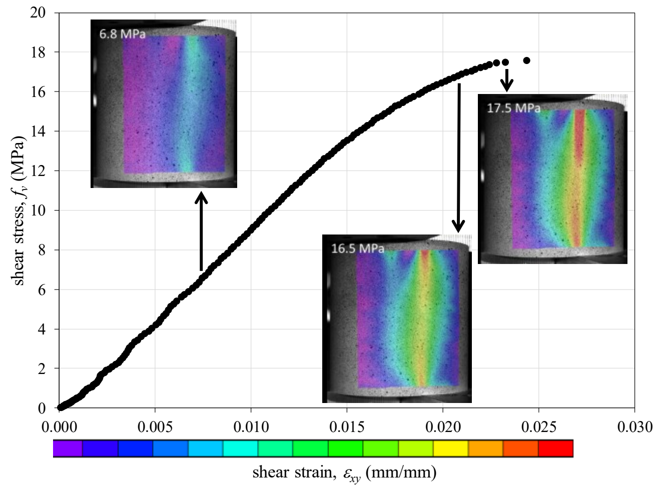

a) shear stress-strain progression of internode shear test

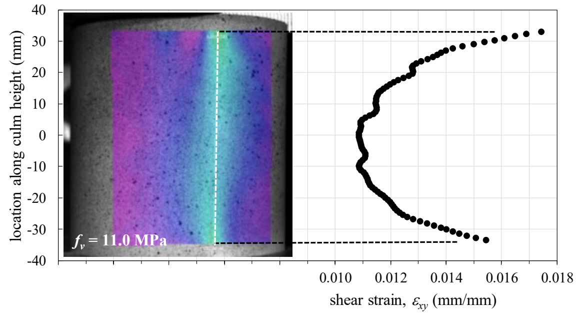

b) shear strain distribution in internode specimen at shear stress = 11.0 MPa

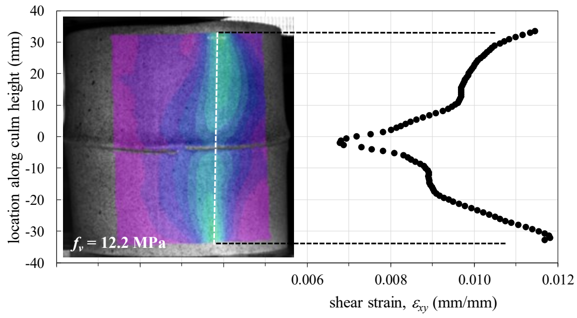

c) shear strain distribution in specimen with node at shear stress = 12.2 MPa

Figure 3 Representative results of longitudinal "bowtie" shear test.

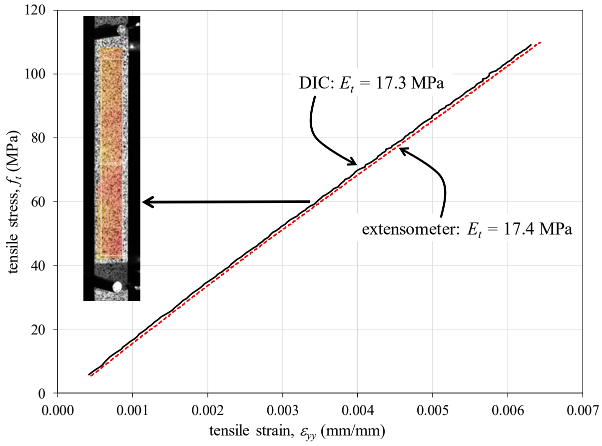

a) comparison between DIC and extensometer derived longitudinal stress-strain curve for internode specimen

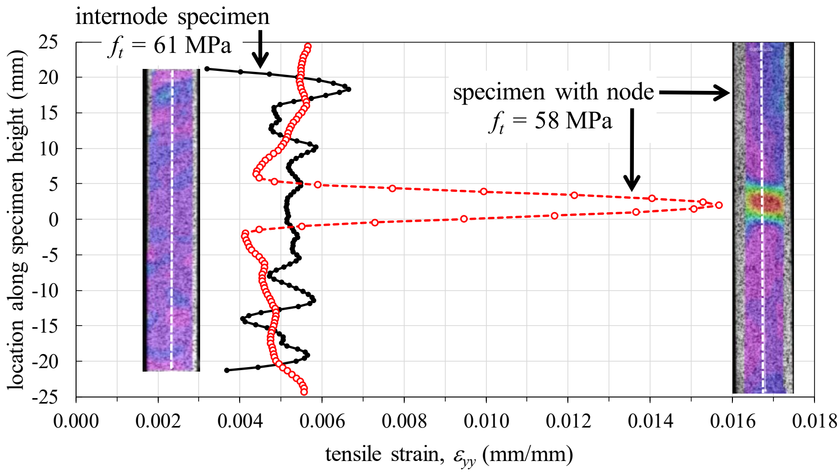

b) longitudinal strain distribution in specimens with and without nodes

Figure 4 Representative results of tension test.

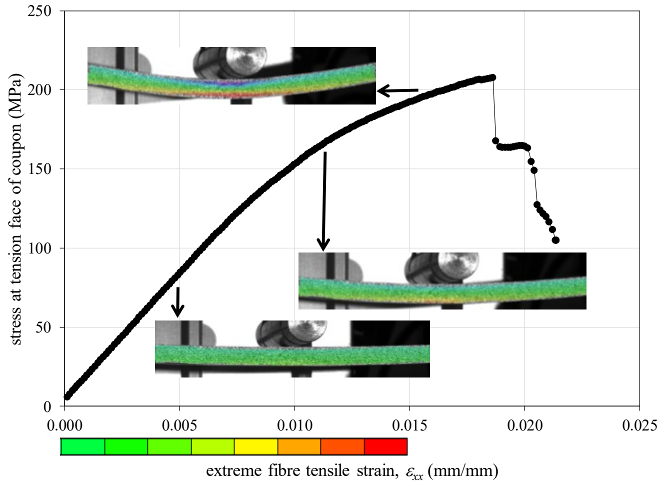

a) longitudunal shear stress-strain progression of OC internode coupon test

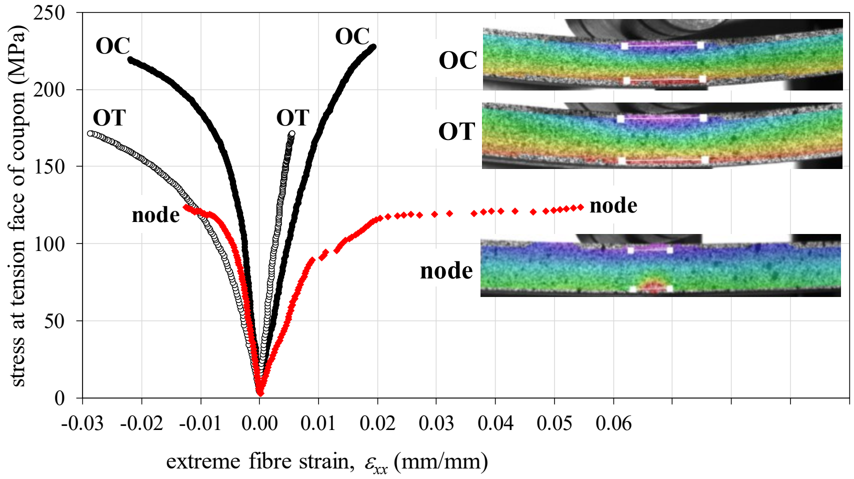

b) longitudinal strain distribution in coupon bending tests

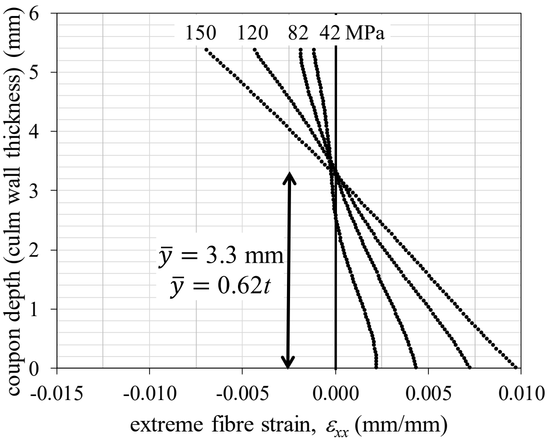

c) strain distributions through depth of OC coupon

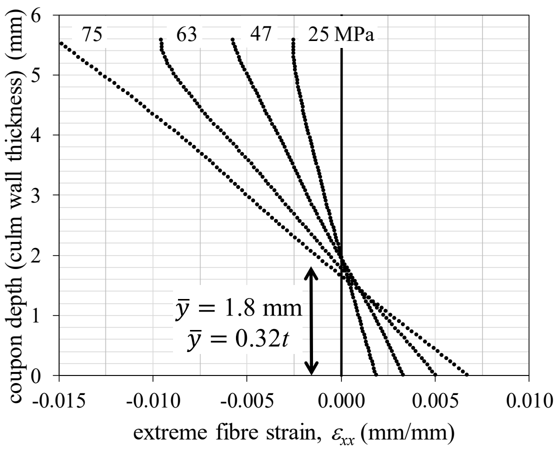

d) strain distributions through depth of OT coupon

Figure 5 Representative results of three-point coupon bending test.

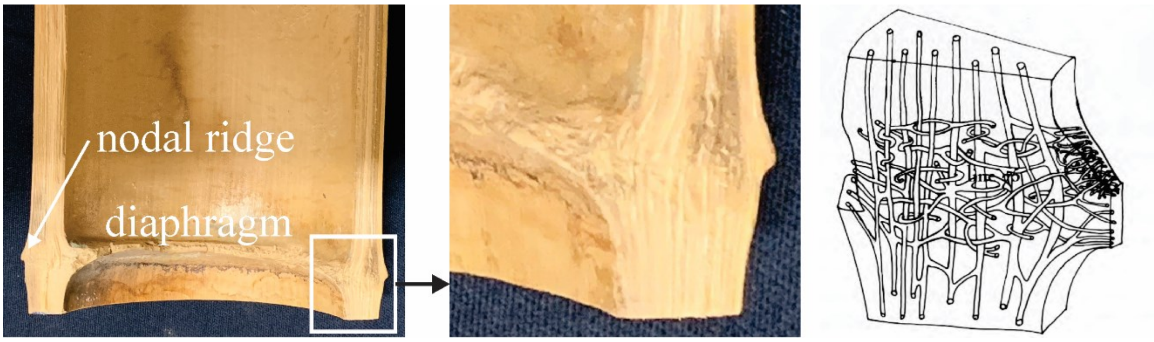

a) nodal region of *P. edulis* showing fibre orientation and local thickening of culm wall

b) skeleton of vascular bundle at node (Liese 1998)

Figure 6 Fibre morphology at node.

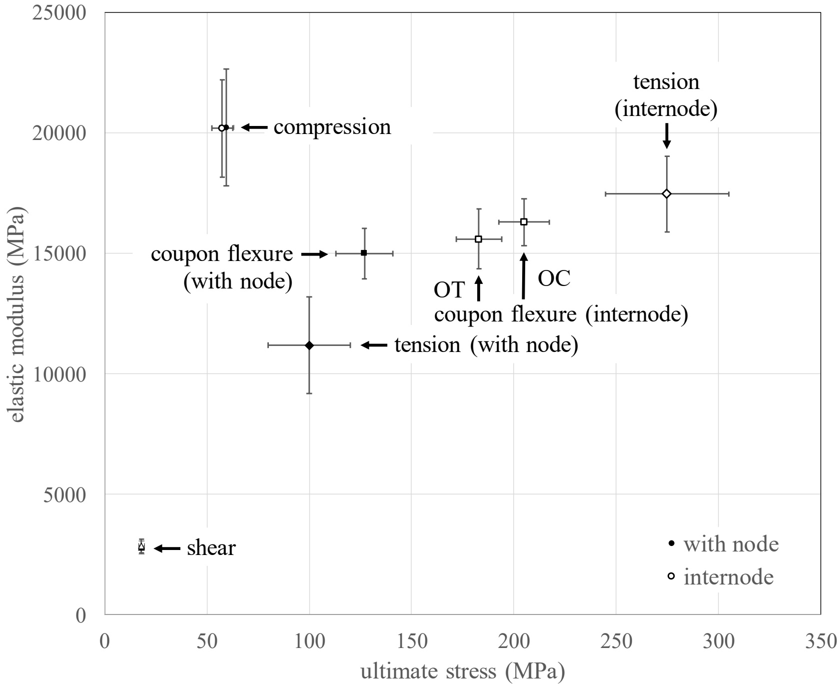

Figure 7 Mechanical characterisation of *P edulis*: strength and modulus (bars indicate one standard deviation in all cases)